

1 **Resource allocation to growth or luxury consumption drives**

2 **mycorrhizal responses**

3

4 Rohan C. Riley - Hawkesbury Institute for the Environment, Western Sydney University,
5 r.riley@westernsydney.edu.au

6 Timothy R. Cavagnaro - The Waite Research Institute and School of Agriculture, Food and
7 Wine, University of Adelaide, timothy.cavagnaro@adelaide.edu.au

8 Chris Brien - The Waite Research Institute and School of Agriculture, Food and Wine,
9 University of Adelaide; Australian Plant Phenomics Facility, The Plant Accelerator,
10 University of Adelaide; Phenomics and Bioinformatics Research Centre, University of
11 South Australia, chris.brien@adelaide.edu.au

12 F. Andrew Smith - The Waite Research Institute and School of Agriculture, Food and Wine,
13 University of Adelaide, andrew.smith@adelaide.edu.au

14 Sally E. Smith - The Waite Research Institute and School of Agriculture, Food and Wine,
15 University of Adelaide, sally.smith@adelaide.edu.au

16 Bettina Berger - The Waite Research Institute and School of Agriculture, Food and Wine,
17 University of Adelaide; Australian Plant Phenomics Facility, The Plant Accelerator,
18 University of Adelaide, bettina.berger@adelaide.edu.au

19 Trevor Garnett - The Waite Research Institute and School of Agriculture, Food and Wine,
20 University of Adelaide; Australian Plant Phenomics Facility, The Plant Accelerator,
21 University of Adelaide, trevor.garnett@adelaide.edu.au

22 Rebecca Stonor - The Waite Research Institute and School of Agriculture, Food and Wine,
23 University of Adelaide, rebecca.stonor@adelaide.edu.au

24 Rhiannon K. Schilling - The Waite Research Institute and School of Agriculture, Food and
25 Wine, University of Adelaide, rhiannon.schilling@adelaide.edu.au

26 Zhong-Hua Chen - Hawkesbury Institute for the Environment, Western Sydney University;

27 School of Science and Health, Western Sydney University,

28 Z.Chen@westernsydney.edu.au

29 Jeff R. Powell - Hawkesbury Institute for the Environment, Western Sydney University,

30 jeff.powell@westernsydney.edu.au

31

32 Running title: Plant strategies drive mycorrhizal phenotypes

33 Keywords: functional traits, plant-microbe interactions, ecosystem function, growth strategy,

34 competition, biodiversity

35 Article type: Letter

36 Number of words, abstract: 150

37 Number of words, main text: 4597

38 Number of references: 61

39 Number of figures: 4 (main text), 6 (supplement)

40 Number of tables: 0 (main text), 2 (supplement)

41 Number of text boxes: 0

42

43 *Corresponding authors: R.C. Riley, email: r.riley@westernsydney.edu.au ; J.R. Powell,

44 email: jeff.powell@westernsydney.edu.au; Hawkesbury Institute for the Environment,

45 Western Sydney University, Locked Bag 1797, Penrith NSW 2751, Australia; P: +61(0)2

46 4570 1093, F: +61(0) 4570 1103

47

48 Statement of Authorship: RCR and JRP conceived and designed the study with help from

49 TRC, FAS, SES, BB, TG, RS, RKS and Z-HC. RCR collected data. RCR and CB analysed

50 data with advice from JRP. RCR wrote the first draft with advice from JRP, and all authors
51 contributed substantially to revisions.

52

53 Data accessibility statement: Data will be made available on Figshare upon publication of the
54 manuscript and the data DOI will be included in the manuscript.

55

56 **Abstract**

57 Highly variable phenotypic responses in mycorrhizal plants challenge our functional
58 understanding of plant-fungal mutualisms. Using non-invasive high-throughput phenotyping,
59 we observed that arbuscular mycorrhizal (AM) fungi relieved phosphorus (P) limitation and
60 enhanced growth of *Brachypodium distachyon* under P-limited conditions, while
61 photosynthetic limitation under low nitrogen (N) was exacerbated by the fungus. However,
62 these responses were strongly dependent on host genotype: only the faster growing genotype
63 (Bd3-1) utilised P transferred from the fungus to achieve improved growth under P-limited
64 conditions. Under low N, the slower growing genotype (Bd21) had a carbon and N surplus
65 that was linked to a less negative growth response compared with the faster growing
66 genotype. These responses were linked to the regulation of N:P stoichiometry, couples
67 resource allocation to growth or luxury consumption in diverse plant lineages. Our results
68 attest strongly to a mechanism in plants by which plant genotype-specific resource economics
69 drive phenotypic outcomes during AM symbioses.

70

71

72

73

74

75 **Introduction**

76 Arbuscular mycorrhizal (AM) fungi are generally considered beneficial associates, improving
77 host-plant access to and uptake of nutrients such as nitrogen and phosphorus (Smith and Read
78 2008). However, several studies have demonstrated that mycorrhizal growth responses
79 (MGRs; the response of plants to growing in the presence of mycorrhizal fungi compared to
80 growth in their absence) can range widely, from positive to negative, and can be difficult to
81 predict (Johnson *et al.* 1997; Klironomos 2003). Several models propose that this context
82 dependency may be explained by dynamics of resource exchange between plants and fungi
83 under light and/or nutrient limiting conditions and that these dynamics may support the
84 maintenance of AM associations for many plant species (Johnson *et al.* 1997; Kiers and van
85 der Heijden 2006; Johnson *et al.* 2015; Walder and van der Heijden 2015; Kiers *et al.* 2016;
86 van der Heijden and Walder 2016). One hypothesis links plant nitrogen (N) and phosphorus
87 (P) limitation and the mycorrhizal carbon (C) source-sink balance to variation in MGRs
88 (Johnson *et al.* 2015). Under low available soil P, an AM fungus can scavenge P and transfer
89 this to the plant, alleviating P deficiency and causing positive MGRs. However, under low N,
90 they may compete for plant-available N, contribute to further N deficiency and cause
91 reductions in C-assimilation, thus yielding negative MGRs (Johnson *et al.* 2015). Given that
92 AM fungi are ubiquitous in terrestrial ecosystems and associate with the majority of plant
93 species, including all important cereal crop species, it is critical to understand what factors
94 drive the context dependency of MGRs and, particularly, observed variation among plant
95 genotypes (Hetrick *et al.* 1996; Klironomos 2003; van der Heijden *et al.* 2004).

96

97 There is likely a genetic basis for variation in MGRs (Kaeppeler *et al.* 2000, Lehnert *et al.*

98 2018). Evidence suggests that mechanisms maintaining the symbiosis may have been

99 selected against by plant domestication and modern crop-breeding approaches, resulting in

100 MGRs that can be positive but small or possibly even negative (Hetrick *et al.* 1992; Zhu *et al.*

101 2001; Sawers *et al.* 2008; Plett *et al.* 2016). In natural ecosystems, AM fungi can influence
102 plant community structure and function (van der Heijden *et al.* 1998; Hartnett and Wilson
103 2002; O'Connor *et al.* 2002), hypothesised to be due to variation in mycorrhizal
104 responsiveness depending on the subordinate-dominance rank of plant community members
105 (Urcelay and Díaz 2003). The latter has been associated with functional processes that
106 underly plant growth, including resource economic trade-offs (Elser *et al.* 2010) and
107 stoichiometric relationships between N and P within individual plants (Yu *et al.* 2010; Yu *et*
108 *al.* 2011; Johnson *et al.* 2015; Yang *et al.* 2016). Therefore, variation in MGRs between
109 plants may be driven by mechanisms constraining plant C, N and P allocation among various
110 tissues (including associated mycorrhizal fungi).

111

112 In plants, the regulation of C, N and P uptake and allocation to various functional processes is
113 closely interconnected due to the central role that these elements have in plant growth and
114 development (Martin *et al.* 2002; Hermans *et al.* 2006). The balance of C, N and P within
115 organisms – known as ecological stoichiometry – is an important determinant of plant
116 biodiversity and ecosystem function (Wright *et al.* 2004; Elser *et al.* 2010; Yu *et al.* 2015;
117 Mariotte *et al.* 2017) and has been linked to plant responses to AM fungi (Johnson *et al.*
118 2015; Yang *et al.* 2016; Mariotte *et al.* 2017). The flexibility of N:P stoichiometry is the
119 physiological tendency of an organism to maintain constant tissue N:P over variation in
120 supply N:P (Sturner and Elser 2002; Persson *et al.* 2010). This tendency can be measured by
121 an index of N:P homeostasis ($H_{N:P}$; the degree to which tissue N:P follows supply N:P
122 changes) – as the degree of homeostasis decreases, the rate that tissue N:P follows supply
123 N:P increases. When both N and P are co-limiting growth, N:P ratios at maximum growth
124 rate tend to converge on the ‘Redfield ratio’ (7.3:1 mass ratio, 16:1 molar ratio) because of an
125 optimal coupling of protein and ribosome production to support high-growth (Elser 2010,
126 Ågren *et al.* 2012). In plants and algae, resources tend to be consumed in excess when N or P
127 supplies are non-limiting for growth. This ‘luxury consumption’ (Lambers and Poorter 2004)

128 causes tissue N:P ratios to follow supply N:P and results in lower $H_{N:P}$. However, when
129 resources are limiting, variation in functional traits such as growth rate may determine $H_{N:P}$
130 because growth depends on the coupled synthesis of ribosomes and proteins. As a result, at
131 low N and P supply, plants with faster growth rates may have N:P ratios that are constrained
132 within a narrower range, resulting in greater $H_{N:P}$. Under non-limiting conditions, plants with
133 slower growth rates and effective nutrient retention strategies may have N and P
134 concentrations that are decoupled from protein and ribosome synthesis, resulting in flexible
135 N:P ratios and a lower $H_{N:P}$ (Sterner and Elser 2002; Persson *et al.* 2010; Sistla and Schimel
136 2012). Therefore, the extent that a plant experiences N or P limitation may be a function of
137 the environmental supply of N and P as well as genotype-dependent functional traits that
138 together determine $H_{N:P}$. We hypothesised that across a finite N:P supply gradient, variation
139 in $H_{N:P}$ between genotypes would be linked to the resource limitation phenotypes that drive
140 MGRs.

141

142 We tested our hypothesis using two accessions of the cereal model *Brachypodium distachyon*
143 (Brutnell *et al.* 2015) that we identified as possibly having contrasting patterns of N and P
144 allocation to growth and, therefore, variable $H_{N:P}$. Both are diploid inbred lines originating
145 from Iraq (Vogel *et al.* 2006). In previous work, accession Bd3-1 was observed to be a larger
146 plant at maturity, with more positive root growth response to N deficiency (Ingram *et al.*
147 2012) and had lower C and N containing metabolite concentrations compared to accession
148 Bd21 (Ingram *et al.* 2012; Shi *et al.* 2015). We predicted that under low P, a plant with a
149 higher $H_{N:P}$ would exhibit faster growth and use additional P in the presence of AM fungi,
150 leading to a more positive MGR than a plant with a lower $H_{N:P}$. However, under low N,
151 additional demand for C and N in the presence of AM fungi will trade-off more with plant
152 growth for a faster growing plant with higher $H_{N:P}$ compared to a slower growing plant with
153 lower $H_{N:P}$. Therefore, when comparing responses between low N supply and low P supply

154 conditions, we expected that the plant with a greater $H_{N:P}$ would have a larger range of MGRs
155 compared to a plant with lower $H_{N:P}$ (Fig. S1).

156

157 ***Materials and Methods***

158 ***Plant growth conditions***

159 AM fungal inoculum was obtained from a wheat field in Coomandook, South Australia (SA)
160 and cultured with maize (*Zea mays* L.). Soil was collected from the same site of origin as the
161 AM inoculum, sterilised by autoclaving twice and diluted by 80% (w/w) with dry sand (N40
162 from Sloans Sands, SA, Australia) to reduce nutrient availability (available P = 8.8 mg/kg,
163 available N = 17.2 mg/kg). We created three N:P supply treatments with the following
164 nutrient combinations: additional N (+52.2 mg/kg NH_4NO_3 of dry soil; +N-P treatment),
165 additional P (+35.4 mg/kg of dry soil; -N+P treatment), and no additional N or P (-N-P
166 treatment). Additional nutrients were added to all pots as described in the Supplemental
167 Methods.

168

169 Three inocula were generated from the original inoculum: a live inoculum, a mock inoculum,
170 and microbial wash. The mock inoculum was generated by autoclaving the live inoculum
171 twice, while the microbial wash was created by mixing live inoculum with water (1:6 w/v),
172 mixing for 15 min and filtering through a 38 μm sieve. Additionally, a second microbial wash
173 was made in the same way using unsterilised field soil. At the time of potting, live inoculum
174 (AM+) or mock inoculum (AM-) was added to each pot by weighing out 1,320 g dry soil and
175 100 g dry inoculum and mixing by hand for 45 s. All pots received 20 mL of each microbial
176 wash. Seeds of *B. distachyon* were surface sterilised in 10% bleach solution and thoroughly
177 rinsed in reverse osmosis (RO) water.

178

179 The experiment was conducted at the Australian Plant Phenomics Facility at the University of
180 Adelaide, SA, using a Scanalyzer 3D system (LemnaTec GmbH, Aachen, Germany) which
181 enabled daily non-destructive red-green-blue (RGB) imaging (one top-view and two side-
182 view images) and daily watering-to-weight (70% water holding capacity). The experiment
183 commenced at the start of October 2016 (i.e. Austral spring) when there were approximately
184 12 h of daylight. Average daily maximum (at midday) irradiance throughout the experiment
185 was 780 $\mu\text{mol}/\text{m}^2/\text{s}$, which is sufficient to support optimal growth of *B. distachyon* (Matos et
186 al. 2014). The average daily light integral was 19 $\text{mol}/\text{m}^2/\text{d}$. Glasshouse conditions were set
187 at 25°C day/ 20°C night and relative humidity was set at 70% throughout the experiment.
188 After 20 days of growth, plants were loaded onto the conveyor system. For each genotype,
189 there were six treatment combinations each replicated six times, except for one treatment
190 where a plant died early into growth. For the final 26 days, plants were imaged and watered-
191 to-weight daily by the Scanalyser 3D system.

192

193 ***Plant harvest and tissue elemental analysis, and root staining***

194 At harvest (day 47) shoots were removed and weighed, then oven-dried at 70°C for 48 h to
195 obtain dry weight. Shoots were ground to a fine powder and analysed for total P using a
196 PANalytical Epsilon 3^x X-Ray Fluorometer (Malvern Panalytical, United Kingdom) and C
197 and N using 40 mg of tissue in an elemental analyser (Flash EA 1112 Series CHN analyser,
198 Thermo-Finnigan, Waltham, MA, USA). Over three days, roots were washed and
199 subsampled for fungal staining by haphazardly selecting fine roots from throughout the root
200 system and storing in 30% ethanol (v/v). The remaining root tissue was oven dried at 70°C
201 for 48 h. Roots were stained for quantification of fungal colonisation using a modified

202 version of the ink-vinegar method (Vierheilig *et al.* 1998) and percent root length colonised
203 assessed using the grid-line intersect method (McGonigle *et al.* 1990).

204

205 ***Data processing, trait calculations and statistical analyses***

206 Using the RGB images, we calculated projected shoot area (PSA), absolute growth rate
207 (AGR), and hue angle (HA; a measure of greenness) according to methods previously
208 described (Neilson *et al.* 2015; Al-Tamimi *et al.* 2016). Tissue N:P ratios are expressed on a
209 mass basis. We calculated the stoichiometric homeostasis coefficient, separately for each
210 genotype under AM+ and AM- treatments, using the inverse of the slope of the line of log-
211 shoot N:P as a response of log-supply N:P (Sternler and Elser 2002; Elser *et al.* 2010).

212 Mycorrhizal growth responses (MGRs) were calculated using PSA of individual AM+
213 (=AM) plants and mean PSA of AM- (=NM) plants using the equation, $100[(AM - \text{mean NM}) / \text{mean NM}]$ (Cavagnaro *et al.* 2003). Shoot area mass ratio (SAMR; PSA per fresh
214 shoot fresh mass) was expressed on a fresh-weight basis. Total weight (g), shoot weight (g),
215 root weight (g), and root mass fraction (RMF) were expressed as a dry mass basis, unless
216 otherwise specified. Plant HA values were extracted from the day of AGR_{max} of each pot for
217 the principal component analysis (PCA) or from the final day before harvest for the percent
218 colonisation analysis. PCA of plant traits and significance testing were conducted using the
219 *rda* and *adonis* functions from the 'vegan' library (Oksanen *et al.* 2013) in R (R Core
220 Development Team 2017), using standardised trait values and Euclidean distances.

222 Univariate mixed models were fit using the R libraries 'ASReml-R' versions 3 (Butler *et al.*
223 2009) and 4 (Butler 2017) and 'asremlPlus' (Brien 2017). To produce PSA and AGR growth
224 curves, a longitudinal mixed-model analysis was performed for PSA (Brien and Demetrio
225 2009) while other trait data were analysed using a mixed model of the same general form
226 (Supplemental Methods).

227

228 **Results**

229 ***Phenotypic responses to nutrient treatments and AM fungi***

230 All responses are summarised in Tables S1 and S2 and summaries of hypothesis tests are
231 presented in Table S3. Projected shoot area (PSA) was strongly correlated with shoot fresh
232 weight ($R^2=0.95$) and dry weight ($R^2=0.93$) at harvest (Fig. S2), confirming its use as a proxy
233 for plant biomass (35–37). While Bd3-1 exhibited a greater average maximum absolute
234 growth rate (AGR_{max}) and PSA than Bd21, the differences were dependent on both the
235 nutrient and fungal treatments (Fig. 1). In the absence of AM fungi, PSA and AGR_{max} of both
236 genotypes responded positively to N addition (+N-P), while addition of P (-N+P) was not
237 observed to increase shoot growth and lead to earlier declines in PSA and absolute growth
238 rate (AGR). Shoot N:P was less than the Redfield ratio when grown in the unfertilised
239 treatment and decreased further when phosphorus was added (Fig. S3), suggesting that N
240 limitation prevented a growth response to P addition. Shoot N:P was greater than the Redfield
241 ratio when nitrogen was added (Fig. S3), suggesting that P limitation was induced once N
242 deficiency was addressed.

243

244 Inoculation with AM fungi resulted in reduced PSA and AGR in the -N+P and -N-P
245 treatments indicating that AM fungi caused growth depressions when plants were N deficient.
246 This growth depression was larger in Bd3-1 compared to Bd21. Bd3-1 had more positive
247 MGRs under -N+P and more negative MGRs under -N-P and +N-P compared to Bd21 (Fig.
248 1c; $P_{genotype:nutrient} = 0.003$).

249

250 ***Genotypes have differences in growth and luxury consumption in response to*** 251 ***nutrient treatments and AM fungi***

252 Principal components analysis (PCA) revealed that shoot trait responses were driven by
253 genotype-specific responses to changing N availability and to AM fungi (Fig. 2). All main

254 effects and interactions were statistically significant ($P < 0.01$) except the three-way
255 interaction, which was marginally nonsignificant ($P_{\text{genotype:nutrient:AM}} = 0.06$), and the genotype-
256 by-AM interaction, which was clearly not significant ($P_{\text{genotype:AM}} > 0.1$). Plants grown in the
257 absence of N addition (-N-P and -N+P) treatments, had negative values and plants grown
258 with added N (+N-P) had positive values along the first axis. Total shoot N (TN) was
259 strongly positively loaded along this axis and shoot area mass ratio (SAMR) was strongly
260 negatively loaded. Shoot P concentration and root mass fraction (RMF) loaded moderately
261 negatively while PSA, HA, shoot N concentration and shoot C concentration loaded
262 moderately positively. Inoculating with AM fungi resulted in a negative shift in loadings
263 along the first axis, this shift was larger in the absence of added N and was greater for Bd3-1
264 than for Bd21. Taken together, these trait responses suggest that AM fungi exacerbated N
265 deficiency and that this may have been stronger in the fast-growing genotype, Bd3-1, than in
266 the slower growing genotype, Bd21.

267

268 The PCA also revealed genotypic differences in growth and shoot concentrations of C, N and
269 P. Across the nutrient treatments, Bd21 tended to have greater C, N, and P concentrations
270 than Bd3-1, while Bd3-1 tended to have higher RMF, PSA, and AGR_{max} . This indicated that
271 Bd21 accumulated more C, N and P but grew less compared to Bd3-1, which invested more
272 C, N and P into growth.

273

274 ***N and P allocation to growth or luxury consumption are determinants of $H_{N:P}$***

275 When plotting tissue N:P against supply N:P across the three nutrient treatments to calculate
276 $H_{N:P}$, we found that Bd3-1 had a more constant tissue N:P as supply N:P changed (higher
277 $H_{N:P}$) compared to Bd21 (Fig. 3a, Fig. S3; $P_{\text{genotype:log(NP Supply)}} < 0.001$). We constructed a new
278 PCA that included traits associated with C assimilation and growth (*i.e.*, C concentration,
279 SAMR, AGR_{max} , PSA, and HA; Fig. S4) and plotted the first axis against shoot N:P ratios of

280 both genotypes to reveal that Bd3-1 had a larger range in trait responses compared to Bd21
281 (Fig. 3b; $P_{\text{genotype:tissue NP}} < 0.001$). Plants that had added N (+N-P) had high values on the first
282 axis and N:P ratios at or above 7.3:1, while plants that were N deficient (-N-P and -N+P) had
283 N:P ratios below 7.3:1. Moreover, Bd3-1 had N:P ratios closer to the Redfield ratio of 7.3:1,
284 which is the ratio where tissue N and P concentrations have been observed to be associated
285 with maximum growth (Sterner and Elser 2002; Ågren *et al.* 2012), in every nutrient
286 treatment compared to Bd21.

287

288 We also observed that, in the presence of AM fungi, shoot N:P ratios were slightly less
289 flexible in both genotypes, as indicated by a greater $H_{N:P}$ (Fig. 3a; $P_{\text{AM:log(NP supply)}} = 0.038$,
290 $P_{\text{AM:nutrient}} = 0.056$). This was driven by the presence of AM fungi resulting in a slightly larger
291 decrease of shoot N:P ratios at higher supply N:P ratios.

292

293 ***C, N and P allocations to growth or luxury consumption are linked to MGRs***

294 Under added N, as N:P ratios approached the Redfield ratio, PSA increased in both genotypes
295 (Fig. 3c; $P_{\text{tissue NP}} < 0.001$) but more so for Bd3-1 ($P_{\text{genotype:tissue NP}} = 0.004$). The addition of
296 AM fungi resulted in more shoot P in both genotypes (Shoot P concentration: $P_{\text{AM:nutrient}} =$
297 0.016; Total shoot P; $P_{\text{AM:nutrient}} < 0.001$). This resulted in a negative shift in the N:P ratios
298 towards the Redfield ratio. However, in Bd3-1 N:P ratios shifted to a mean of 7.3:1 along
299 with a significant increase in PSA, while in Bd21 N:P ratios were larger than 7.3:1 and PSA
300 did not increase (Fig. 3c; $P_{\text{AM:genotype}} = 0.009$).

301

302 Negative MGRs under N deficient conditions were linked to reductions in C and increases in
303 N concentration. Under N deficient conditions, in the absence of AM fungi, Bd3-1 had a
304 greater PSA and lower C and N concentrations than Bd21 (Fig. S5a and b; C concentration:
305 $P_{\text{genotype}} = 0.009$, N concentration: $P_{\text{genotype}} < 0.001$). When AM fungi were added, PSA

306 decreased to a similar level in both genotypes, while C concentration decreased and N
307 concentration increased to an extent that depended on the nutrient treatment and/or genotype
308 (C concentration: $P_{\text{genotype:AM}} = 0.044$, N concentration: $P_{\text{genotype:nutrient:AM}} = 0.033$). This led to
309 AM fungi inducing a greater decrease in C:N ratio in Bd3-1 compared to Bd21 (Fig. S5c;
310 $P_{\text{genotype:AM}} = 0.037$).

311

312 Finally, we observed that increased AM colonisation was exacerbating N deficiency
313 symptoms (Fig. 4, Fig. S6). This was indicated by negative trends in plant HA on day 46
314 (Fig. 4a; $P_{\%col} = 0.006$) and shoot N concentration for both genotypes (Fig. 4b; $P_{\%col} < 0.001$),
315 with no detected differences in the slopes among genotypes ($P_{\%col:genotype} > 0.05$) and nutrient
316 treatments ($P_{\%col:nutrient} > 0.05$). Changes in percent root length colonised were positively
317 correlated with total dry plant weight (Fig. 4c; $P_{\%col} = 0.024$), with no detected difference in

318 slope among genotypes and nutrient treatments ($P_{\%col:genotype} = 0.65$, $P_{\%col:nutrient} = 0.87$,
319 $P_{\%col:genotype:nutrient} = 0.61$).

320

321 **Discussion**

322 Taken together, the results presented here provide a novel framework to investigate plant
323 responses to AM fungi whereby MGRs are driven by the regulation of C, N and P allocation
324 within the plant together with environmental supply of N and P. First, we demonstrate that *B.*
325 *distachyon* stoichiometric flexibility is determined by inherent genotypic differences in N and
326 P allocation to growth or luxury consumption. We also demonstrate that the presence of AM
327 fungi exacerbated N deficiency and increased P uptake to plants, which caused negative and
328 neutral/positive MGRs under N-limiting and P-limiting supply conditions, respectively.

329 Bringing together these observations, we demonstrate that plant genotypic differences in
330 growth and luxury consumption determined the magnitude of these MGRs. By demonstrating
331 this link, we show that plant genotypic differences in resource allocation are an important
332 determinant of phenotypic responses to AM fungi.

333

334 Central to our findings is the growth rate hypothesis, which applies to all organisms and
335 predicts that the coupling of tissue N:P to growth-rate is determined by P-rich ribosomal
336 RNA that is required for the synthesis of N-rich proteins and organelles, in support of growth
337 (Sturner and Elser 2002; Elser *et al.* 2010; Persson *et al.* 2010; Ågren *et al.* 2012; Sistla and
338 Schimel 2012). When both N and P are co-limiting growth, N:P ratios at maximum growth
339 rate tend to converge to 7.3:1 mass ratio because of an optimal coupling of protein and
340 ribosome production to support high-growth (Elser *et al.* 2010; Ågren *et al.* 2012). This was
341 also the ratio in *B. distachyon* where we observed the greatest PSA in our experiment.

342 Moreover, we found that Bd3-1 was faster growing and had a higher degree of N:P

343 homeostasis ($H_{N:P}$) compared to Bd21, which was slower growing and had a lower $H_{N:P}$

344 because it accumulated more N or P. These results are in line with previous observations that
345 rapid growth in plants and algae drives tissue N:P ratios within a narrower range, increasing
346 $H_{N:P}$ because of the coupled use of N and P between ribosomes and proteins. On the other
347 hand, slower growing plants and algae tend to have larger ranges in N:P, decreasing $H_{N:P}$,
348 because of the luxury accumulation of N and P (Elser *et al.* 2010; Persson *et al.* 2010).

349

350 ***Allocations of C, N and P to growth or luxury consumption determine***
351 ***phenotypic responses to AM fungi***

352 We show that the different ranges of MGRs experienced by Bd3-1 and Bd21 across the
353 nutrient treatments were linked to genotypic differences in allocation of N and P to growth or
354 luxury consumption. Under N deficient conditions, we observed evidence of competition for
355 N between AM fungi and plants, with plants obtaining less than their required N as indicated
356 by lower C and N concentrations, HA, PSA, and AGR_{max} and increased SAMR, and RMF
357 when AM fungi were present under N deficient conditions. These responses can be explained
358 by the large proportion of plant N that is present in chlorophyll, leading to reduced
359 chlorophyll production when plant N decreases (Evans 1983). Decreased plant C-gain
360 because of reduced chlorophyll likely resulted in reductions in shoot PSA, while increased
361 RMF suggested greater N scavenging to cope with the N limitation (Hilbert 1990). The larger
362 trait shift in Bd3-1 in the presence of AM fungi under N deficient conditions may be
363 explained by the tendency of Bd3-1 to invest more in growth, possibly allocating N to
364 biomass and chlorophyll, compared to Bd21, which appeared to consume N in excess of what
365 was needed to support growth. Competition with AM fungi for N led to a greater decline in
366 shoot greenness (HA) in Bd3-1, which likely caused a larger decrease in C production and a
367 more negative MGR compared to Bd21.

368

369 However, when N was added, Bd3-1 was better able to use additional P obtained by AM

370 fungi for growth compared to Bd21. This is supported by the observation that the increase in
371 PSA due to AM fungi in Bd3-1 was linked to a greater total shoot P, shift in N:P ratios
372 towards the Redfield ratio along with more growth, while Bd21 also accumulated more total
373 shoot P but maintained higher C, N and P concentrations and did not grow as much. This
374 suggests that under added N, Bd21 was luxury consuming P rather than using it for growth.
375 To confirm these hypotheses, it would be valuable to assess genotype and mycorrhizal
376 responses to N- and P-limitation while also independently constraining photosynthetic
377 capacity, for example, by reducing availability of light (Johnson *et al.* 2015) or atmospheric
378 carbon dioxide (Sage 1995). In addition, assessments of more genotypes exhibiting these and
379 intermediate growth strategies would be valuable to evaluate the shape and strength of
380 relationships between stoichiometric homeostasis and mycorrhizal phenotypes.

381

382 ***Stoichiometric homeostasis may help explain plant responses to AM fungi in***
383 ***managed and natural systems***

384 The functional trait coordination of Bd3-1 and Bd21 supports the notion that the genotypes
385 may be considered more acquisitive and conservative growth strategists, respectively.
386 Acquisitive plants tend to be larger with greater shoot N and P while slower growing
387 conservative plants accumulate resources in excess of their growth demands (Lambers and
388 Poorter 2004; Sistla and Schimel 2012; Mariotte 2014). Bd3-1 also had a greater RMF across
389 the experiment compared to Bd21, which indicates a greater demand for below-ground
390 resources and is consistent with a more acquisitive growth strategy (Lambers and Poorter
391 2004). Importantly, the different strategies employed by plants have been linked to variation
392 in plant community composition. Dominant plants tend to be more acquisitive strategists than
393 subordinates, which tend to be more conservative species (Mariotte 2014). Moreover,

394 dominant plants have been found to have a greater $H_{N:P}$ than subordinate plants species
395 (Mariotte *et al.* 2017).
396
397 Our findings suggest a mechanistic basis for the effects of AM fungi on plants with different
398 growth strategies. Previously, the effect of AM fungi on plant diversity has been suggested to
399 be dependent on the mycorrhizal responsiveness of the dominant and subordinate plant
400 species in the community (Urcelay and Díaz 2003). Under low P, reductions in diversity have
401 been attributed to AM fungi when dominant species are more mycorrhizal responsive than
402 subordinates because the presence of AM fungi intensified competition by enhancing the
403 growth of dominants (Newsham *et al.* 1995; Hartnett and Wilson 2002; O'Connor *et al.*
404 2002). On the other hand, several studies have found that AM fungi increase diversity, which
405 has been proposed to occur when both dominant and subordinate species are mycorrhizal
406 responsive (Grime *et al.* 1987; van der Heijden *et al.* 1998). Mariotte *et al.* (2017)
407 hypothesised that, under low N, subordinate plants benefit more from AM fungi compared to
408 dominant plants because the former have a greater resource surplus that enables C transfer in
409 the absence of a growth depression. Our results support this notion since we found that the
410 MGR was not as negative in the genotype having a greater C and N surplus under low N
411 (Bd21). Our study provides a possible mechanistic explanation for the effect of AM fungi on
412 competitive outcomes between plants. Further studies should explore the link between $H_{N:P}$
413 variability of coexisting plant species and the effect of AM fungi on their competitive
414 outcomes and resulting community structure.

415

416 Our findings apply to agricultural crops as well. In a survey of ten wheat cultivars, Hetrick *et*
417 *al.* (1996) found growth responsiveness of the plants to P was a good indication of
418 mycorrhizal responsiveness and that non-responsive cultivars had significantly higher P
419 concentrations than responsive cultivars. In a similar study using six different wheat
420 cultivars, Zhu *et al.* (2001) found higher P concentrations for inoculated plants and negative
421 MGRs for all cultivars, possibly due to low light conditions, and a negative relationship
422 between growth responsiveness to P and MGRs. These and the current study suggest that P
423 transfer occurs in the presence of AM fungi but growth responsiveness depends on genotype
424 as well as photosynthetic limitation. Future studies should investigate whether mycorrhizal
425 responsiveness in crops is related to resource utilisation for immediate growth versus storage
426 for later use, and the ultimate destination of resources (for example, seed or fruit) in the latter
427 case. This may lead to a better understanding of the determinants of mycorrhizal phenotypes
428 for crop plants.

429

430 This study focused primarily on host plant physiology, but it is probable that fungal
431 physiology is also important in determining plant phenotypic response. We used a mixed
432 community AM inoculum, from an agricultural soil, that likely reflects the norm in nature
433 since single plants are, more often than not, interacting with multiple AM fungal individuals.
434 The effects of individual AM fungi on the MGRs of *B. distachyon* can be variable (Hong *et*
435 *al.* 2012). Previous work suggests that species compositional differences between AM fungal
436 assemblages associated with Bd21 and Bd3-1 are small (Donn *et al.* 2017), but we have little
437 knowledge about functional differences between these assemblages. Resource economic
438 approaches can be applied to understand trade-offs in allocation of resources toward growth,
439 storage, defence and other processes for fungi (Zhang and Elser 2017), and may even help
440 explain variation in how different AM fungal communities may drive different plant growth
441 and development outcomes (Powell and Rillig 2018).

442

443 **Acknowledgements**

444 This research was supported by a postgraduate research internship grant from the Australian
445 Plant Phenomics Facility to RCR and a Discovery Grant from the Australian Research
446 Council to JRP (DP140103936). We thank Jose Barrero for providing seed. We also thank
447 staff at The Plant Accelerator for technical support: Helli Meinecke, Dr Guntur Tankung,
448 George Sainsbury, Evi Guidolin, Robin Hoskins, Lidia Mischis, Nicole Bond, Fiona
449 Groskreutz, Richard Norrish, Rune Gam Hiede Jall. Peter Reich, Jonathan Plett and three
450 anonymous reviewers provided helpful comments on an earlier version of the manuscript.
451 The Plant Accelerator, Australian Plant Phenomics Facility, is supported under the National
452 Collaborative Research Infrastructure Strategy (NCRIS) of the Australian Government.

453

454

455

456 ***Data Availability***

457 Data are accessible at <https://doi.org/10.6084/m9.figshare.8427608>.

458

459

460 **References**

- 461 Ågren, G.I., Wetterstedt, J.Å.M. & Billberger, M.F.K. (2012). Nutrient limitation on
462 terrestrial plant growth – modeling the interaction between nitrogen and phosphorus.
463 *New Phytol*, 194, 953–960.
- 464 Al-Tamimi, N., Brien, C., Oakey, H., Berger, B., Saade, S., Ho, Y.S., *et al.* (2016). Salinity
465 tolerance loci revealed in rice using high-throughput non-invasive phenotyping. *Nat*
466 *Commun*, 7.

467 Brien, C.J. (2017). asremlPlus: Augments the use of ASReml-R in fitting mixed models.
468 Available at: <http://chris.brien.name/rpackages>.

469 Brien, C.J. & Demetrio, C. (2009). Formulating mixed models for experiments, including
470 longitudinal experiments. *J Agric Biol Environ Stat*, 14, 253–280.

471 Brutnell, T.P., Bennetzen, J.L. & Vogel, J.P. (2015). *Brachypodium distachyon* and *Setaria*
472 *viridis*: model genetic systems for the grasses. *Annu Rev Plant Biol*, 66, 465–485.

473 Butler, D., Cullis, B., Gilmour, A. & Gogel, B. (2009). Analysis of Mixed Models for S--
474 language Environments: ASReml--R Reference Manual. Queensland DPI, Brisbane.

475 Butler, D.G. (2017). asreml4: Fits the linear mixed model. Version 4.1.0. Available at:
476 <http://www.vsni.co.uk/>.

477 Cavagnaro, T.R., Smith, F.A., Ayling, S.M. & Smith, S.E. (2003). Growth and phosphorus
478 nutrition of a Paris-type arbuscular mycorrhizal symbiosis. *New Phytol*, 157, 127–134.

479 Donn, S., Kawasaki, A., Delroy, B., Chochois, V., Watt, M. & Powell, J.R. (2017). Root type
480 is not an important driver of mycorrhizal colonisation in *Brachypodium distachyon*.
481 *Pedobiologia*, 65, 5–15.

482 Elser, J.J., Fagan, W.F., Kerkhoff, A.J., Swenson, N.G. & Enquist, B.J. (2010). Biological
483 stoichiometry of plant production: metabolism, scaling and ecological response to
484 global change. *New Phytol*, 186, 593–608.

485 Evans, J.R. (1983). Nitrogen and photosynthesis in the flag leaf of wheat (*Triticum aestivum*
486 L.). *Plant Physiol*, 72, 297–302.

487 Golzarian, M.R., Frick, R.A., Rajendran, K., Berger, B., Roy, S., Tester, M., *et al.* (2011).
488 Accurate inference of shoot biomass from high-throughput images of cereal plants.
489 *Plant Methods*, 7, 2.

490 Grime, J.P. (2006). *Plant Strategies, Vegetation Processes, and Ecosystem Properties*. John
491 Wiley & Sons, Chichester.

492 Grime, J.P., Mackey, J.M.L., Hillier, S.H. & Read, D.J. (1987). Floristic diversity in a model
493 system using experimental microcosms. *Nature*, 328, 420–422.

494 Hartnett, D.C. & Wilson, G.W.T. (2002). The role of mycorrhizas in plant community
495 structure and dynamics: lessons from grasslands. In: *Diversity and Integration in*
496 *Mycorrhizas, Developments in Plant and Soil Sciences*. Springer, Dordrecht, pp. 319–
497 331.

498 van der Heijden, M.G., Bruin, S. de, Luckerhoff, L., van Logtestijn, R.S. & Schlaeppli, K.
499 (2016). A widespread plant-fungal-bacterial symbiosis promotes plant biodiversity,
500 plant nutrition and seedling recruitment. *ISME J*, 10, 389–399.

501 van der Heijden, M.G.A. & Walder, F. (2016). Reply to ‘Misconceptions on the application
502 of biological market theory to the mycorrhizal symbiosis.’ *Nature Plants*, 2, 16062.

503 Hermans, C., Hammond, J.P., White, P.J. & Verbruggen, N. (2006). How do plants respond
504 to nutrient shortage by biomass allocation? *Trends Plant Sci*, 11, 610–617.

505 Hetrick, B., Wilson, G. & Cox, T. (1992). Mycorrhizal dependence of modern wheat
506 varieties, landraces, and ancestors. *Can J Bot*, 70, 2032–2040.

507 Hetrick, B.A.D., Wilson, G.W.T. & Todd, T.C. (1996). Mycorrhizal response in wheat
508 cultivars: relationship to phosphorus. *Can J Bot*, 74, 19–25.

509 Hilbert, D.W. (1990). Optimization of plant root: shoot ratios and internal nitrogen
510 concentration. *Annals of Botany*, 66, 91–99.

511 Hong, J.J., Park, Y.-S., Bravo, A., Bhattarai, K.K., Daniels, D.A. & Harrison, M.J. (2012).
512 Diversity of morphology and function in arbuscular mycorrhizal symbioses in
513 *Brachypodium distachyon*. *Planta*, 236, 851–865.

514 Honsdorf, N., March, T.J., Berger, B., Tester, M. & Pillen, K. (2014). High-throughput
515 phenotyping to detect drought tolerance QTL in wild barley introgression lines. *PLoS*
516 *One*, 9, e97047.

517 Ingram, P.A., Zhu, J., Shariff, A., Davis, I.W., Benfey, P.N. & Elich, T. (2012). High-
518 throughput imaging and analysis of root system architecture in *Brachypodium*

519 *distachyon* under differential nutrient availability. *Philos Trans R Soc Lond B Biol Sci*,
520 367, 1559–1569.

521 Johnson, N.C., Graham, J.H. & Smith, F.A. (1997). Functioning of mycorrhizal associations
522 along the mutualism–parasitism continuum. *New Phytol*, 135, 575–585.

523 Johnson, N.C., Wilson, G.W.T., Wilson, J.A., Miller, R.M. & Bowker, M.A. (2015).
524 Mycorrhizal phenotypes and the Law of the Minimum. *New Phytol*, 205, 1473–1484.

525 Kaeppler, S.M., Parke, J.L., Mueller, S.M., Senior, L., Stuber, C. & Tracy, W.F. (2000).
526 Variation among maize inbred lines and detection of quantitative trait loci for growth at
527 low phosphorus and responsiveness to arbuscular mycorrhizal fungi. *Crop Sci*, 40, 358–
528 364.

529 Kiers, E.T. & van der Heijden, M.G.A. van der. (2006). Mutualistic stability in the arbuscular
530 mycorrhizal symbiosis: exploring hypotheses of evolutionary cooperation. *Ecology*, 87,
531 1627–1636.

532 Kiers, E.T., West, S.A., Wyatt, G.A.K., Gardner, A., Bücking, H. & Werner, G.D.A. (2016).
533 Misconceptions on the application of biological market theory to the mycorrhizal
534 symbiosis. *Nature Plants*, 2, 16063.

535 Klironomos, J.N. (2003). Variation in plant response to native and exotic arbuscular
536 mycorrhizal fungi. *Ecology*, 84, 2292–2301.

537 Lambers, H. & Poorter, H. (2004). Inherent variation in growth rate between higher plants: A
538 search for physiological causes and ecological consequences. *Adv Ecol Res*, 34, 283–
539 362.

540 Lehnert, H., Serfling, A., Friedt, W. & Ordon, F. (2018). Genome-wide association studies
541 reveal genomic regions associated with the response of wheat (*Triticum aestivum* L.) to
542 mycorrhizae under drought stress conditions. *Front Plant Sci*, 9, 1728.

543 Mariotte, P. (2014). Do subordinate species punch above their weight? Evidence from above-
544 and below-ground. *New Phytol*, 203, 16–21.

545 Mariotte, P., Canarini, A. & Dijkstra, F.A. (2017). Stoichiometric N:P flexibility and
546 mycorrhizal symbiosis favour plant resistance against drought. *J Ecol*.

547 Martin, T., Oswald, O. & Graham, I.A. (2002). *Arabidopsis* seedling growth, storage lipid
548 mobilization, and photosynthetic gene expression are regulated by carbon:nitrogen
549 availability. *Plant Physiol*, 128, 472–481.

550 Matos, D.A., Cole, B.J., Whitney, I.P., MacKinnon, K.J.-M., Kay, S.A. & Hazen, S.P.
551 (2014). Daily changes in temperature, not the circadian clock, regulate growth rate in
552 *Brachypodium distachyon*. *PLoS ONE*, 9, e100072.

553 McGonigle, T.P., Miller, M.H., Evans, D.G., Fairchild, G.L. & Swan, J.A. (1990). A new
554 method which gives an objective measure of colonization of roots by vesicular-
555 arbuscular mycorrhizal fungi. *New Phytol*, 115, 495–501.

556 Neilson, E.H., Edwards, A.M., Blomstedt, C.K., Berger, B., Møller, B.L. & Gleadow, R.M.
557 (2015). Utilization of a high-throughput shoot imaging system to examine the dynamic
558 phenotypic responses of a C₄ cereal crop plant to nitrogen and water deficiency over
559 time. *J Exp Bot*, 66, 1817–1832.

560 Newsham, K., Watkinson, A., West, H. & Fitter, A. (1995). Symbiotic fungi determine plant
561 community structure: changes in a lichen-rich community induced by fungicide
562 application. *Funct Ecol*, 442–447.

563 O'Connor, P.J., Smith, S.E. & Smith, F.A. (2002). Arbuscular mycorrhizas influence plant
564 diversity and community structure in a semiarid herbland. *New Phytol*, 154, 209–218.

565 Oksanen, J., Blanchet, F.G., Kindt, R., Legendre, P., Minchin, P.R., O'hara, R., *et al.* (2013).
566 *vegan: Community Ecology Package*. R package. [https://CRAN.R-](https://CRAN.R-project.org/package=vegan)
567 [project.org/package=vegan](https://CRAN.R-project.org/package=vegan)

568 Persson, J., Fink, P., Goto, A., Hood, J.M., Jonas, J. & Kato, S. (2010). To be or not to be
569 what you eat: regulation of stoichiometric homeostasis among autotrophs and
570 heterotrophs. *Oikos*, 119, 741–751.

571 Plett, J.M., Plett, K.L., Bithell, S.L., Mitchell, C., Moore, K., Powell, J.R., *et al.* (2016).
572 improved *Phytophthora* resistance in commercial chickpea (*Cicer arietinum*) varieties
573 negatively impacts symbiotic gene signalling and symbiotic potential in some varieties.
574 *Plant Cell Environ*, 39, 1858–1869.

575 Powell, J.R. & Rillig, M.C. (2018). Biodiversity of arbuscular mycorrhizal fungi and
576 ecosystem function. *New Phytol*, 220, 1059–1075.

577 R Core Development Team. (2017). *R: A language and environment for statistical*
578 *computing*. Vienna.

579 Sage, R.F. (1995). Was low atmospheric CO₂ during the Pleistocene a limiting factor for the
580 origin of agriculture? *Glob Chang Biol*, 1, 93–106.

581 Sawers, R.J.H., Gutjahr, C. & Paszkowski, U. (2008). Cereal mycorrhiza: an ancient
582 symbiosis in modern agriculture. *Trends Plant Sci*, 13, 93–97.

583 Shi, H., Ye, T., Song, B., Qi, X. & Chan, Z. (2015). Comparative physiological and
584 metabolomic responses of four *Brachypodium distachyon* varieties contrasting in
585 drought stress resistance. *Acta Physiol Plant*, 37, 122.

586 Sistla, S.A. & Schimel, J.P. (2012). Stoichiometric flexibility as a regulator of carbon and
587 nutrient cycling in terrestrial ecosystems under change. *New Phytol*, 196, 68–78.

588 Smith, S.E. & Read, D.J. (2008). *Mycorrhizal Symbiosis*. Academic Press, Amsterdam.

589 Sterner, R.W. & Elser, J.J. (2002). *Ecological Stoichiometry: The Biology of Elements from*
590 *Molecules to the Biosphere*. Princeton University Press, Princeton.

591 Urcelay, C. & Díaz, S. (2003). The mycorrhizal dependence of subordinates determines the
592 effect of arbuscular mycorrhizal fungi on plant diversity. *Ecol Lett*, 6, 388–391.

593 Vierheilig, H., Coughlan, A.P., Wyss, U. & Piché, Y. (1998). Ink and vinegar, a Simple
594 staining technique for arbuscular-mycorrhizal fungi. *Appl Environ Microbiol*, 64, 5004–
595 5007.

596 Vogel, J.P., Garvin, D.F., Leong, O.M. & Hayden, D.M. (2006). *Agrobacterium*-mediated
597 transformation and inbred line development in the model grass *Brachypodium*
598 *distachyon*. *Plant Cell Tiss Organ Cult*, 84, 199–211.

599 Walder, F. & van der Heijden, M.G.A. (2015). Regulation of resource exchange in the
600 arbuscular mycorrhizal symbiosis. *Nature Plants*, 1, 15159.

601 Wright, I.J., Reich, P.B., Westoby, M., Ackerly, D.D., Baruch, Z., Bongers, F., *et al.* (2004).
602 The worldwide leaf economics spectrum. *Nature*, 428, 821–827.

603 Yang, G., Yang, X., Zhang, W., Wei, Y., Ge, G., Lu, W., *et al.* (2016). Arbuscular
604 mycorrhizal fungi affect plant community structure under various nutrient conditions
605 and stabilize the community productivity. *Oikos*, 125, 576–585.

606 Yu, Q., Chen, Q., Elser, J.J., He, N., Wu, H., Zhang, G., *et al.* (2010). Linking stoichiometric
607 homeostasis with ecosystem structure, functioning and stability. *Ecol Lett*, 13, 1390–
608 1399.

609 Yu, Q., Elser, J.J., He, N., Wu, H., Chen, Q., Zhang, G., *et al.* (2011). Stoichiometric
610 homeostasis of vascular plants in the Inner Mongolia grassland. *Oecologia*, 166, 1–10.

611 Yu, Q., Wilcox, K., Pierre, K.L., Knapp, A.K., Han, X. & Smith, M.D. (2015).
612 Stoichiometric homeostasis predicts plant species dominance, temporal stability, and
613 responses to global change. *Ecology*, 96, 2328–2335.

614 Zhu, Y.-G., Smith, S.E., Barritt, A.R. & Smith, F.A. (2001). Phosphorus (P) efficiencies and
615 mycorrhizal responsiveness of old and modern wheat cultivars. *Plant Soil*, 237, 249–
616 255.

617

618

619 **Main Figures**

620

621 **Fig. 1.** Longitudinal and mycorrhizal growth responses of *Brachypodium distachyon*
622 genotypes to N and P supply. Projected shoot area (PSA) (**A**) and absolute growth rate
623 (AGR) (**B**) plotted against days after planting. Curves were obtained from linear mixed-effect
624 models that included smoothing spline terms for the trends of days after planting. Shaded
625 areas around lines are estimated 95% confidence intervals calculated from the fitted values.
626 **C:** Box-and-whisker plots of the mycorrhizal growth response (MGR) calculated with PSA
627 (at 45 days). $n=6$ per treatment, except for Bd21/AM-/++N-P and Bd21/AM+/++N-P where
628 $n=5$.

629

630 **Fig. 2.** Principal component (PC) analysis of Bd21 and Bd3-1 functional traits. Displayed
631 traits include shoot area - mass ratio (SAMR; fresh projected shoot area / fresh shoot weight);
632 average hue angle (HA); total nitrogen (TN); carbon (C), nitrogen (N) and phosphorus (P)
633 concentrations in shoot tissue; and root mass fraction (RMF; dry root weight / dry total plant
634 weight). Symbols represent group centroids and whiskers represent one standard error.

635

636 **Fig. 3.** The coordination of plant traits in relation to stoichiometric homeostasis. **A:** Log
637 tissue N:P plotted against log supply N:P used to calculate N:P homeostasis coefficients
638 ($H_{N:P} = 1/\text{slope}$ of the relationship) of the genotypes. **B:** the first component axis (PC1)
639 associated with growth- and allocation-associated traits (C concentration, SAMR, AGR_{max} ,
640 PSA, and HA) and **C:** PSA on the day of harvest, each plotted against tissue N:P ratio.
641 Vertical dashed lines indicate a mass N:P ratio of 7.3:1 (molar ratio 16:1) that represents the
642 Redfield ratio. $n=6$ per treatment, except for Bd21/AM-/++N-P and Bd21/AM+/++N-P where
643 $n=5$. Lines were fitted as approximate trends of the true relationships (Table S3). The
644 stoichiometric coefficient values ($H_{N:P}$) were determined from the slope for each treatment

645 combination in the maximal model: Bd3-1/AM- = 5.9, Bd21/AM- = 2.8, Bd3-1/AM+ = 6.4,
646 Bd21/AM+ = 2.9.

647

648 **Fig. 4.** Nitrogen (N) competition revealed in relationships between plant traits and AM fungal
649 root colonisation. The acquisitive (Bd3-1, blue) and conservative (Bd21, red) genotypes are
650 plotted against **A:** hue angle on day 46, **B:** shoot N concentration (mg/g) and **C:** total dry
651 biomass for each nutrient treatment. Lines were fitted as approximations to the trends
652 obtained from mixed model analyses. $n=6$, except for Bd21/AM+/+N-P where $n=5$.

653

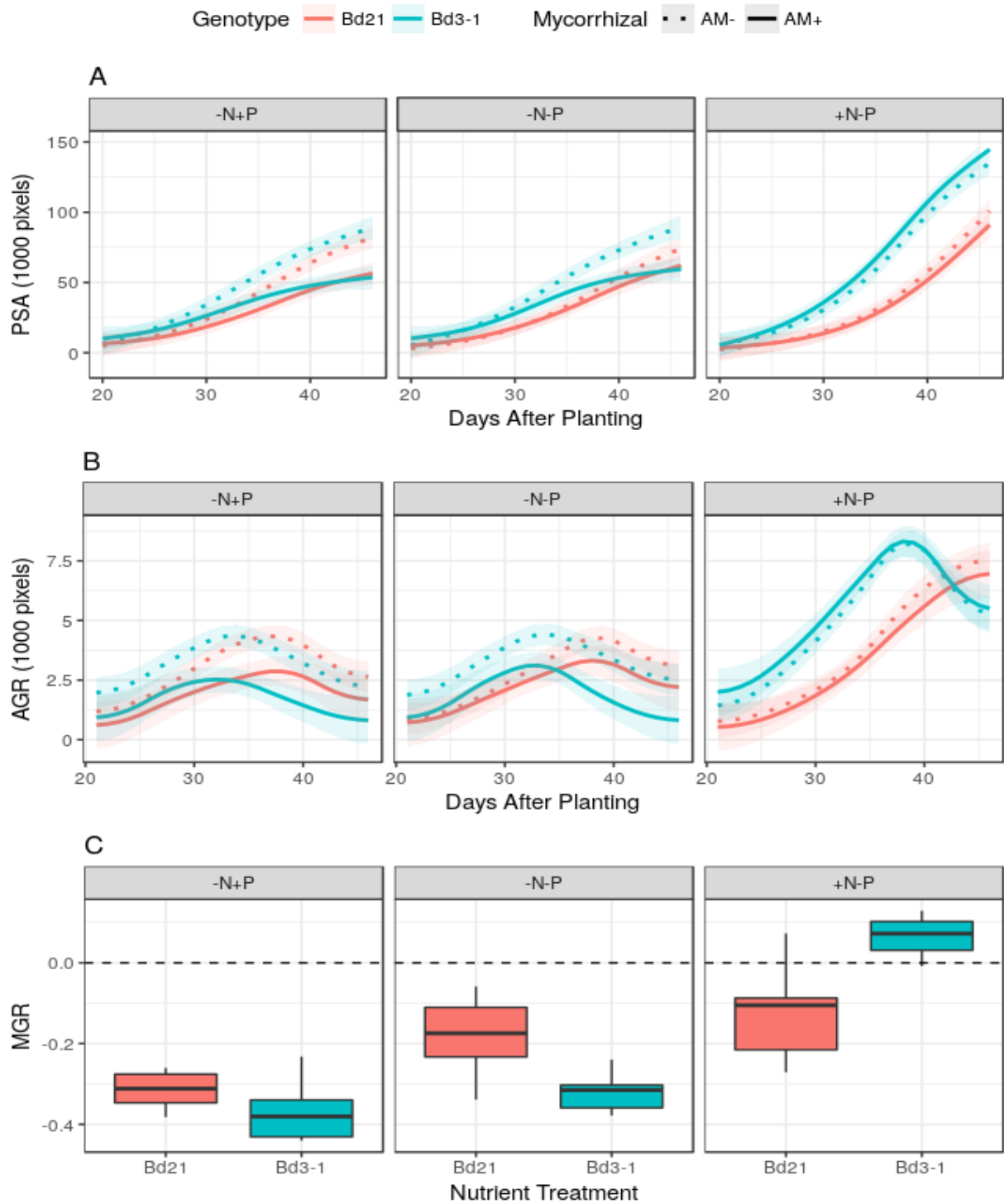
654

655

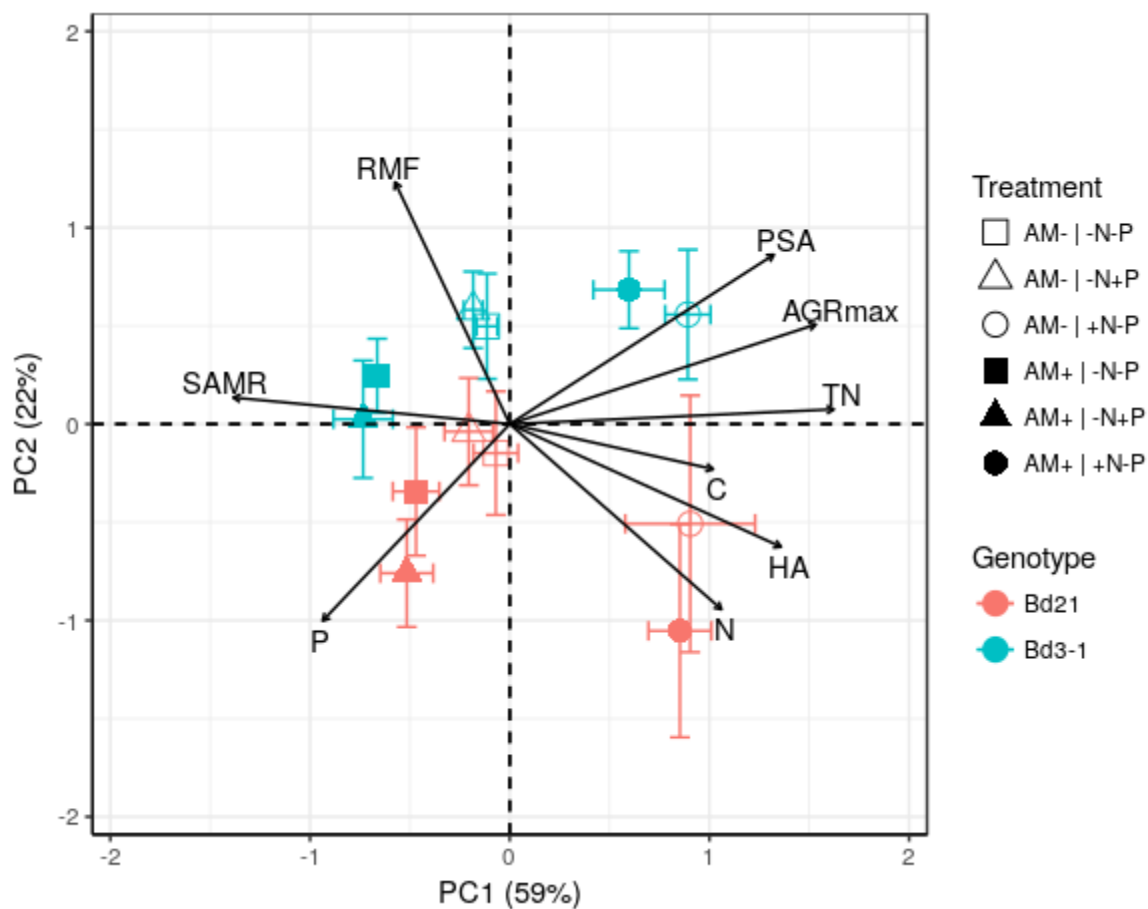
656

657

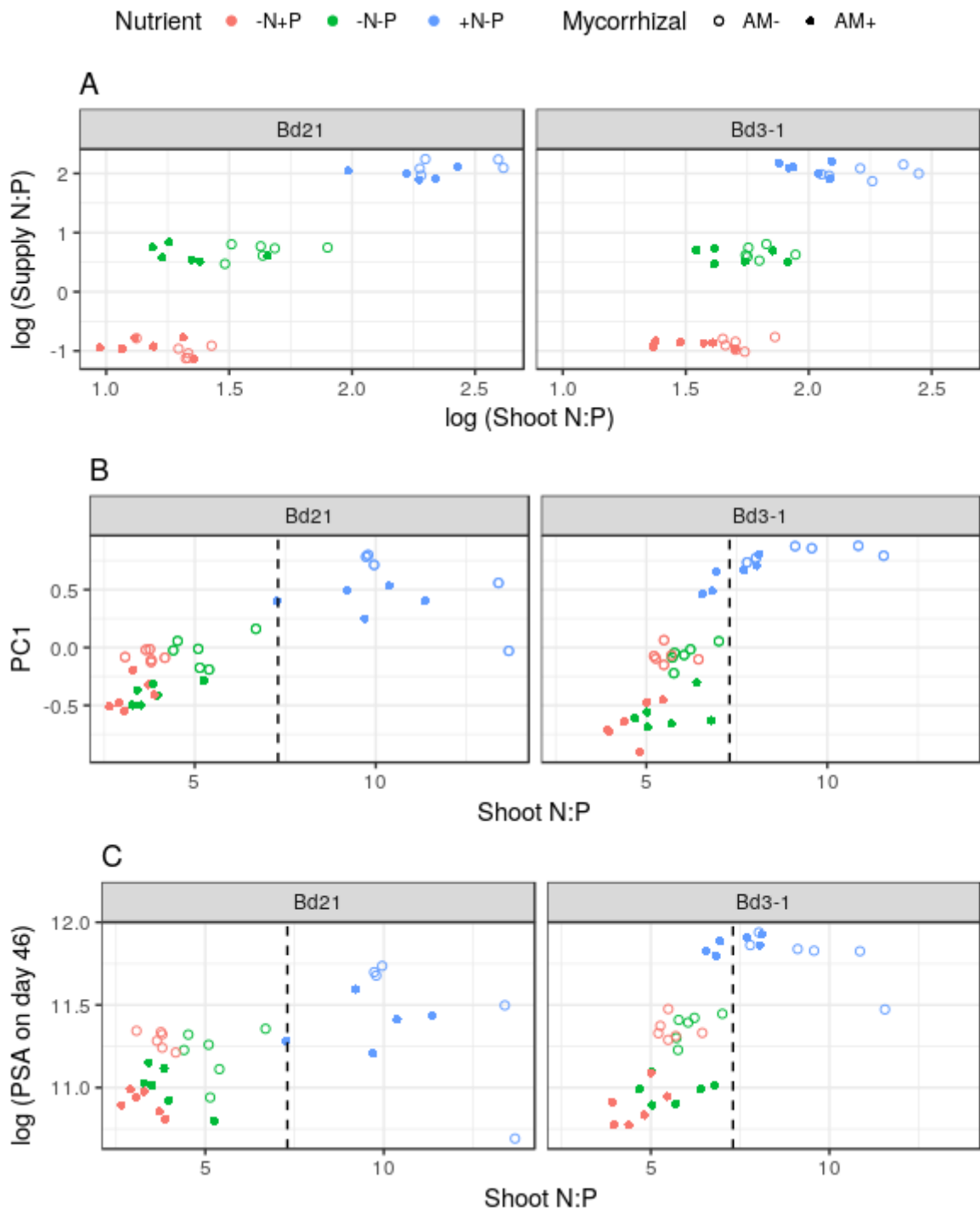
658



661 Fig. 2



662



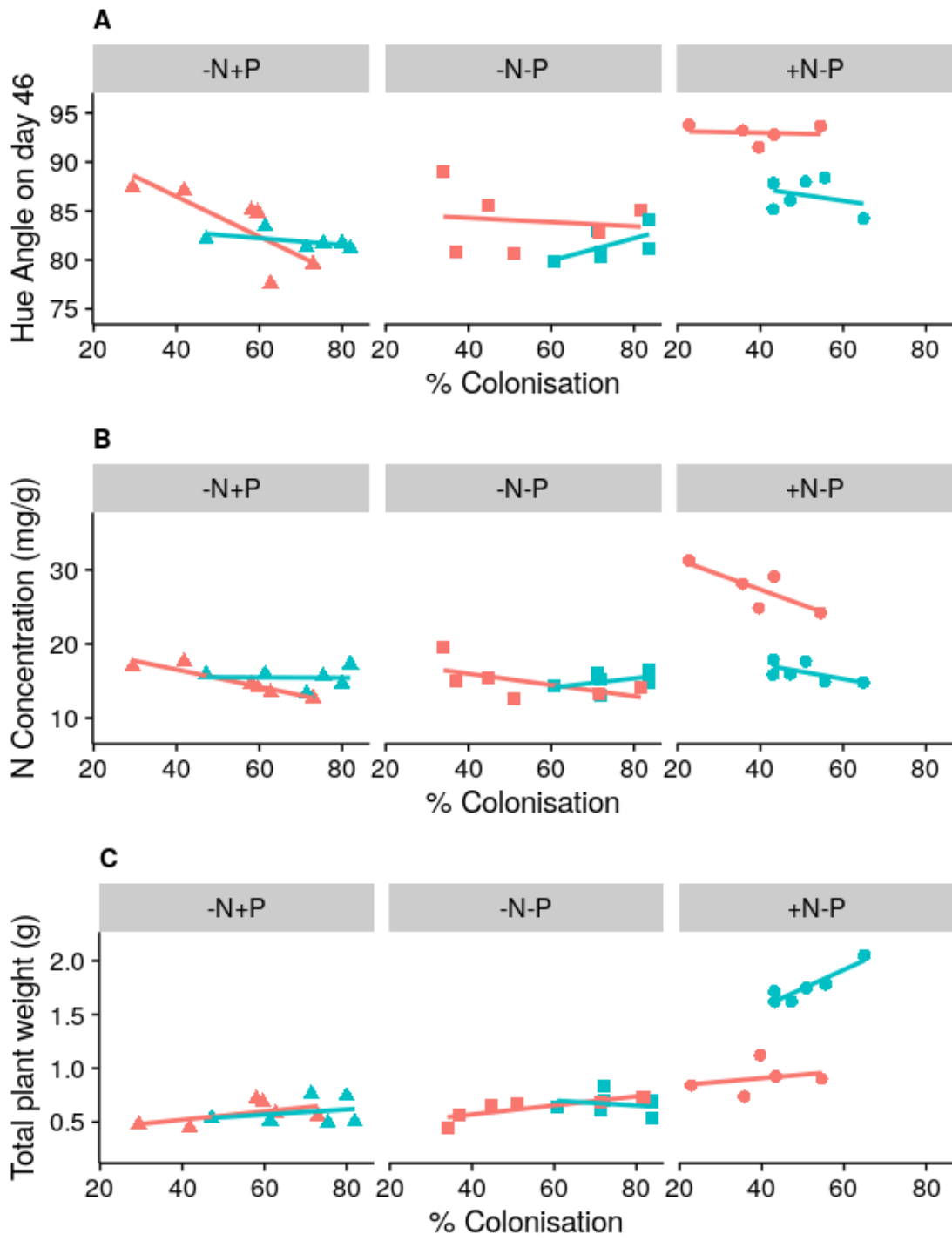
664

665

666

667

668 Fig 4.



669

670